Deep learning-based integration of sequence and structure information for efficient predicting miRNA-drug associations

Nan Sheng, Yunzhi Liu, Ling Gao, Lei Wang, Chenxu Si, Lan Huang,* and Yan Wang*

Key Laboratory of Symbol Computation and Knowledge Engineering of Ministry of Education, College of Computer Science and Technology, Jilin University, ChangChun, 130012, China

E-mail: huanglan@jlu.edu.cn; wy6868@jlu.edu.cn

Abstract

Extensive research has shown that microRNAs (miRNAs) play a crucial role in cancer progression, treatment, and drug resistance. They have been recognized as promising potential therapeutic targets for overcoming drug resistance in cancer treatment. However, limited attention has been paid to predicting association between miRNAs and drugs by computational methods. Existing approaches typically focus on constructing miRNA-drug interaction graph, which may result in their performance being limited by interaction density. In this work, we propose a novel deep learning method that integrates sequence and structural information to infer miRNA-drug associations (MDAs), called DLST-MDA. This approach innovates by utilizing attribute information of miRNAs and drugs instead of relying on the commonly used interaction graph information. Specifically, considering the sequence lengths of miRNAs and drugs, DLST-MDA employs multi-scale convolutional neural network (CNN) to learn sequence embeddings at

different granularity levels from miRNA and drug sequences. Additionally, it leverages the power of graph neural networks to capture structural information from drug molecular graphs, providing a more representation analysis of the drug features. To evaluate DLST-MDA's effectiveness, we manually constructed a benchmark dataset for various experiments based on the latest databases. Results indicate that DLST-MDA performs better than other state-of-the-art methods. Furthermore, case studies of three common anticancer drugs can evidence the usefulness in discovering novel MDAs. The data and source code are released at https://github.com/sheng-n/DLST-MDA.

Introduction

Cancer remains a leading cause of death worldwide, with rising incidence and mortality threatening human health.[1] Despite chemotherapy being the primary treatment for cancer patients, its effectiveness is compromised by emerging drug resistance, leading to treatment failure and disease recurrence. Recent studies have shed light on the crucial role of miRNAs (small non-coding RNAs of 19-25 nucleotides) in cancer development and progression, revealing their potential as targets for therapy and their close relationship to drug resistance.[2,3] For example, it has been demonstrated that miR-20a inhibits the expression of cylindromatosis, thereby promoting cisplatin resistance in gastric cancer, suggesting that regulating the expression of miR-20a may be a potential therapeutic strategy for oppose chemotherapy resistance in gastric cancer.[4] Recent evidence has shown that miRNA-93 can regulate gemcitabine resistance in pancreatic cancer cells by targeting the PTEN-mediated PI3K/Akt signaling pathway.[5] More importantly, some miRNAs can also serve as potential therapeutic targets for enhancing drug sensitivity. For instance, miR-200c increases doxorubicin sensitivity in breast cancer cells by reducing MDR1 gene expression.[6] Furthermore, miR-107 enhances the efficacy of cisplatin against resistant gastric cancer cells by modulating the HMGA2/mTOR/P-gp pathway, thereby increasing sensitivity to the chemotherapeutic agent.[7] This renders it a promising therapeutic target for enhancing cisplatin sensitivity in

gastric cancer treatment. Therefore, uncovering miRNA-drug relationships facilitates drug development and the rational use of clinical therapeutic strategies.

Traditional laboratory experiments to infer these relationships are time-consuming and labor-intensive. Consequently, designing computational methods to address this issue is a promising avenue for accelerating research. Recent advancements in biochemical technologies have facilitated numerous laboratory experiments, confirming that many miRNAs are closely associated with anticancer drugs. These findings have contributed to the rapid growth of databases documenting associations between miRNAs and drugs. For example, NoncoRNA is a database that has manually curated experimentally supported non-coding RNA-related drugs from biomedical literature.[8] This resource has been instrumental in investigating drug sensitivity and resistance-associated ncRNA in human cancers. Another notable resource is the ncRNADrug database, recently constructed by Cao et al.[9] This integrated and comprehensive platform documents both manually organized and computationally predicted ncRNA-drug associations. Additionally, it provides information on potential drug combinations for treating resistant cancers. This wealth of available data has enabled the advancement of computational methods to efficiently identify miRNA-mediated drugs.

In recent years, computational methods based on deep learning and graph neural networks have been widely applied to molecular association prediction, such as disease-associated non-coding RNAs,[10–12] and drug repositioning.[13,14] Additionally, a few computational approaches have been developed to identify the relationships miRNA-mediated drug resistance or sensitivity. Most of them are graph-based approaches, for example, Huang et al. integrated miRNA expression profiles, drug structures, disease ontology, and known miRNA-drug associations information to extract node embedding, employing an end-to-end graph convolution network (GCN) for predicting the miRNA-associated drug resistance.[15] By constructing a ncRNA-drug resistance bipartite graph based on known association, Li et al. presented a linear residual GCN for predicting ncRNAs-drug associations.[16] Niu et al. utilized miRNA-drug bipartite graph and combinations of different miRNA and drug feature as inputs to the

GCN to extract node potential representations and perform drug resistance prediction.[17] Wang et al. introduced a dual network matrix factorization-based approach that leverages similarities between small molecules and miRNAs to infer their associations.[18] Deng et al. built a miRNA-drug heterogeneous network by integrating miRNA and drug similarities and MDAs. Then, a dual-channel heterogeneous graph neural network was applied to extract node embedding and obtain potential miRNA-related drug sensitivity.[19] Wei et al. presented a computational model with graph collaborative filtering algorithm to infer miRNA-drug sensitivity on a build bipartite graph.[20] Recently, Zhou et al. developed graph autoencoder that uses random path masking to learn miRNA and drug features from miRNA-drug heterogeneous graphs and reconstruct association scores.[21] Ou et al. developed an graph approach that employs meta-path to extract subnetwork features from miRNA-drug heterogeneous graph, subsequently integrating node information through hypergraph contrastive learning and attention mechanisms.[22] Fan et al. proposed a computational framework that constructs ncRNA-drug heterogeneous graph based on existing ncRNA data, utilizing LightGCN for node feature extraction and view contrastive learning to derive drug resistance association scores.[23] Li et al. integrated miRNA sequence similarity, drug structure similarity, and miRNA/drug gaussian interaction profile kernel similarity and combined them with principal component analysis to extract nodal features.[24] Despite the remarkable success, these methods tend to have certain limitations: the scarcity of annotated miRNA-drug association data and the presence of numerous negative samples, which are susceptible to the interaction graph density when extracting features and predicting on such a sparse and noisy association network. In addition, there is still lack of comprehensive public benchmark datasets documenting miRNA-mediated drugs.

To overcome the aforementioned challenges, we curate a benchmark dataset of association between miRNAs and drugs, and presents a deep learning-based framework (DLST-MDA) that integrates sequence and structure information for MDA prediction. Our approach utilizes multi-scale CNN as sequence encoder, preserving rich sequence information. Addition-

ally, we designed GCN-based encoder to capture and leverage complex structural information from drug molecular graphs. The contributions of our work can be summarized as follows:

- The propose DLST-MDA, a deep learning framework that integrates sequence and structural information to predict miRNA-mediated drugs. Unlike previous approaches that mainly rely on interaction graph information, DLST-MDA extract features directly from the attribute information of miRNAs and drugs.

- Considering the length of miRNA sequences and drug SMILES strings, DLST-MDA employes multi-scale CNN as encoders, which can effectively capture sequence information at different granularity levels. Furthermore, we introduce drug molecular graphs to capture the structural information of drugs using GCN, which can enhance the prediction capability by incorporating spatial and chemical properties of drugs into the model.

- We conduct extensive experiments on a manually constructed benchmark dataset, and our proposed DLST-MDA outperforms the baseline methods, demonstrating the effectiveness of DLST-MDA in all aspects.

Materials and methods

Benchmark datasets

The MDA data were curated from the ncRNADrug database, a comprehensive resource published in 2023, which records experimentally confirmed ncRNAs related to drug resistance/sensitivity.[9] In this study, we downloaded and selected experimentally validated associations (miRNA-associated drug resistance and sensitivity) between miRNAs and drugs, excluding associations involving non-miRNAs. Furthermore, we filtered miRNAs that have been deleted in miRBase v22[25] (as of April 2024), and drugs with unknown annotation. Finally, a benchmark dataset comprising 8720 miRNA-drug associations, involving 1578

miRNAs and 156 drugs, was available for analysis. The miRNA mature sequences and drug SMILES were gained from the miRBase v22 and DrugBank v5.1.12[26] (as of April 2024), respectively, based on their miRNA names and DrugBank IDs. For this dataset, 98% of the miRNA sequences were less than 24, and 83% of the drug SMILES were less than 100 in length (as shown in Figure 1). Consequently, the maximum lengths of miRNA and drug SMILES were chosen to be 24 and 100 for the training and test sets in this study, respectively.

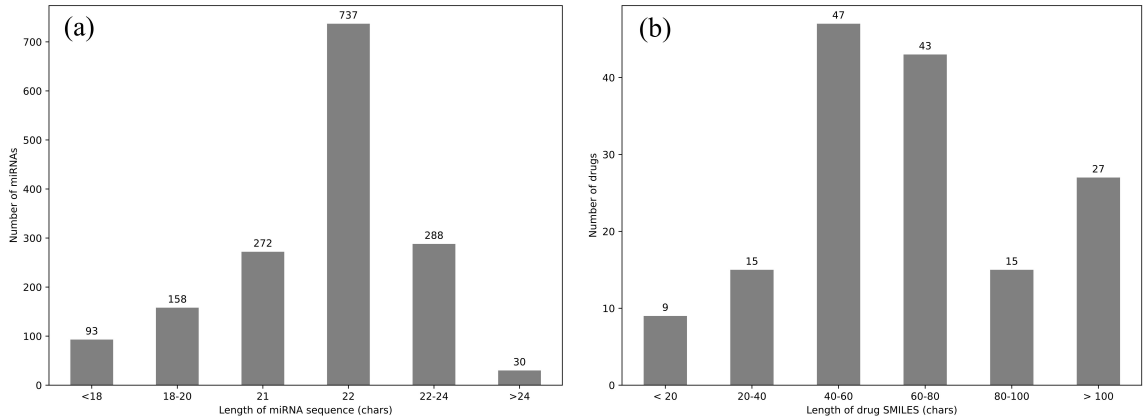

Figure 1: Length distribution of (a) miRNA sequences and (b) drug SMILES strings.

Overview of DLST-MDA

The proposed DLST-MDA architecture is depicted in Figure 2. Specifically, the architecture comprises three main components: (1) miRNA encoder network: a multi-scale CNN module for extracting features from given miRNA sequence. (2) drug encoder network: a hybrid module that combining multi-scale CNN and graph neural network for extracting drug representations from given drug two modalities (drug SMILES and molecular graphs). (3) Association prediction: a module for predicting the likelihood of miRNA-drug binding affinity. Next, we describe the technical details of each key component.

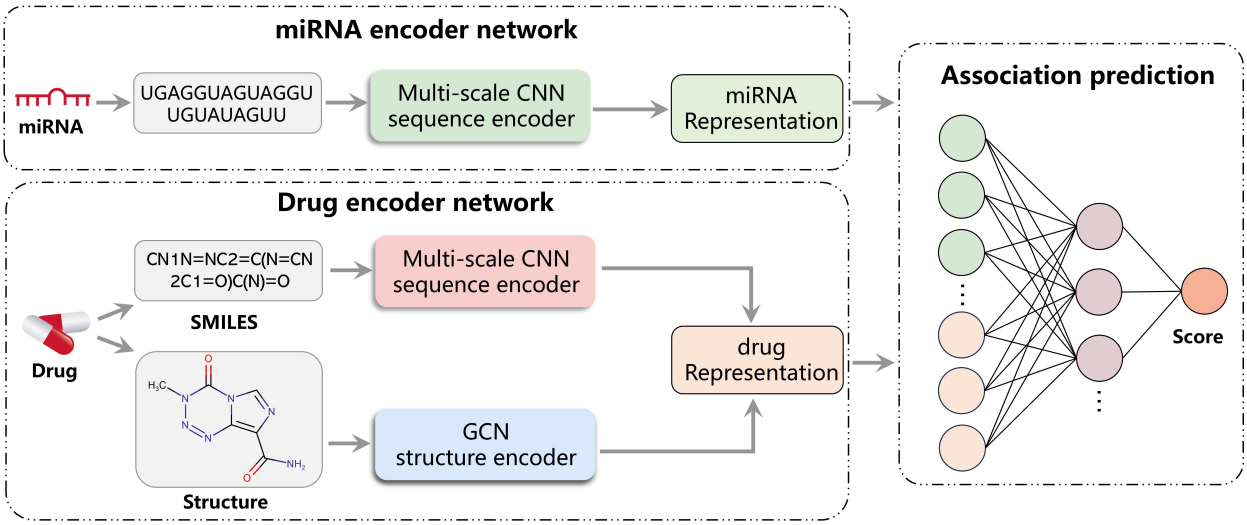

Figure 2: Overview of the proposed DLST-MDA.

miRNA encoder network

miRNA representation

Given a miRNA sequence, it is comprised of 4 base types (A, G, C, U). The ordered bases of miRNA can be regarded as words of sentences in the field of natural language processing. Therefore, in this study, one-hot encoding is adopted to present the miRNA sequence. Through this approach, each miRNA sequence is encoded as two-dimensional matrix of $L \times 4$, where L denotes the sequence length of the miRNA, and 4 presents the size of the base symbol dictionary. As mentioned previously, 98% of the miRNA sequences in this dataset were less than 24 nucleotides (nt) in length. To facilitate the training process, sequences are adjusted to a uniform length of 24 by cutting or padding with zeros. These sequences are then fed into an sequence embedding layer, producing a miRNA embedding matrix $M \in \Re^{N_m \times em}$, where N_m and em represent the sequence length and embedding dimension of the miRNA, respectively.

Multi-scale CNN sequence encoder

In general, convolutional filters of different scales have been shown to extract diverse granularity features. Considering for miRNA sequence, which are characteristically short (typically 20-25 nt in length), deeper networks do not always yield superior performance. In light of this, we propose a CNN module based on multi-scale strategy. Specifically, the multi-scale CNN block incorporates three branches with distinct convolution kernels, each comprising of two 1D-CNN convolutional layers and one max-pooling layer. The convolutional layer contains a group of trainable filters that encode local features within their receptive fields by convolving with the input. The max-pooling layer down-samples the output from the previous layer without utilizing any learnable parameters. For DLST-MDA, the miRNA embedding matrix $M \in \Re^{N_m \times em}$ is fed into multi-scale CNN to learn feature map at various levels. Subsequently, these feature maps are fused to obtain the miRNA sequences representation $Z_M \in \Re^{dm \times 1}$, where dm denotes the final learned embedding dimension. This multi-scale approach allows for the capture of both fine-grained and broader contextual information from the miRNA sequences, potentially leading to more robust and information representations.

$$Z_M = concat\left(CNN_i\left(M, W_{m_i}, k\right)\right), k = 2, 3, 4 \tag{1}$$

where k and i represents convolutional kernel size and CNN branch, respectively. W_{m_i} denotes the weight matrix for that branch.

Drug encoder network

Drug representation

Simplified Molecular Input Line Entry System (SMILES) is a concise and widely-used method for describing drug molecules as strings of characters. Let $d = \{d_1, d_2, \cdots d_{N_d}\}$ denote the drug compounds, where d_i represents an atom or a structure indicator, N_d indicates the drug length. For this study, we set maximum compound length to 100, padding shorter

strings with zeros to fix the uniform length. The drug sequence is first processed through a character embedding layer, transforming it into a drug embedding matrix $D \in \Re^{N_d \times ed}$, where ed denotes the embedding dimension. However, this encoding scheme has a significant limitation: it fails to capture enough structural relatedness between different atoms with the molecule. To enrich drug feature extraction, molecular graphs are utilized to describe drug molecules. Specifically, a drug is represented by a molecular graph $G_d = (V_d, E_d)$, where each node $\alpha_i \in V_d$ denotes an atom in the drug, and each edge $e_{i,j} \in E_d$ represents a chemical bond between atoms α_i and α_j. In addition, we also used RDKit to generate the drug feature matrix X_d, including atomic features such as element type, atomic degree, aromaticity, and other relevant physicochemical properties.

Multi-scale CNN sequence and GCN structure encoder

Similar to miRNA, the drug SMILES sequence is encoded into a sequence representation vector $Z_{DS} \in \Re^{dd_s \times 1}$ using an independent multi-scale CNN block. This block consists of two 1D-CNN layers and one max-pooling layer. Graph neural networks have emerged as the leading method for graph-related tasks, including node and graph classification. Their strength lies in automatically capturing potential features by aggregating node neighborhoods and attributes information. The drug molecule graph encoder takes $G_d = (V_d, E_d)$ as input and learns an F-dimensional node representation for each atom. In this study, we employ GCN, which is a powerful variant of graph neural networks and is widely used as feature extractors for various graph data.[27] It's important to note that the original GCN produces node-level feature vectors, but predicting miRNA-related drugs requires graph-level representations of each drug. Our experiments indicate that the max-pooling typically achieves superior performance compared to aggregated graph-level feature methods such as sum and averaging for this task.

$$Z_D = Z_{DS} + Z_{DT} \tag{2}$$

Formally, given a drug molecular graph $G_d = (V_d, E_d)$, its adjacency matrix A_d and node features X_d serve as input for each drug. In this study, we implement a three-layer GCN, which can be formulated as:

$$Z_{DT_n} = \hat{A}\sigma\left(\hat{A}\sigma\left(\hat{A}X_dW_0\right)W_1\right)W_2 \tag{3}$$

where $\hat{A} = \widehat{D}^{-\frac{1}{2}}(A_d + I)\widehat{D}^{-\frac{1}{2}}$ denotes the normalized adjacency matrix, I is an identity matrix, and $\widehat{D}$ is a diagonal matrix. σ represent the ReLU activation function and W are learnable parameter weight matrices for each layer. However, the GCN model learns the node-level output Z_{DT_n}. To adapt GCN for learning the global graph representation vector, we incorporate a max-pooling layer after the final GCN layer, resulting the graph representation vector $Z_{DT} \in \Re^{dd_t \times 1}$. Finally, we concatenate drug sequence feature Z_{DS} and the structural feature Z_{DT} to get the final drug feature representation $Z_D \in \Re^{dd \times 1}$, where dd denotes the final drug embedding dimension.

Association prediction

By applying miRNA and drug encoder networks, we obtain the final learned embeddings Z_M and Z_D for miRNAs and drugs, respectively. These embeddings are then concatenated to predict the interactions strength of them. Specifically, the prediction module consists of two-layer fully connected neural network (FCNN). The output layer produces a probability score $\hat{y}$, which indicates the likelihood of an interaction between the input miRNA and drug molecule. As this is framed as a binary classification task, the overall MDA prediction model DLST-MDA is trained with binary cross-entropy loss function:

$$\text{loss} = -[y\log(\hat{y}) + (1-y)\log(1-\hat{y})] \tag{4}$$

where y denotes the truth interaction label, "1" indicates that the input miRNA interacts with the input drug and "0" indicates that there is no interaction.

Experiments and Results

Experimental setups and evaluation metrics

Parameter settings: DLST-MDA is implemented using PyTorch, a popular deep learning framework. The development environment includes NumPy v1.24.3, PyTorch v2.3.0, scikit-learn v1.3.2, and PyTorch-Geometric v2.5.3. All experiments are executed on a system equipped with the GeForce RTX 3060 graphic card. For optimization, an Adam optimizer with the learning rate of 0.0005 is employed and train the model for 30 epochs. The input embeddings $em(ed)$ have size of 64, representing each character in sequences and SMILES as a 64-dimensional dense vector. Multi-scale CNN block comprises three parallel branches, each containing two stacked 1D-CNNs and one max-pooling layer. The 1D-CNN window sizes for each branch are set to 2, 3 and 4 for miRNA (drug), respectively. The model encodes miRNAs and drugs with an embedding dimension (dm, dd) of 128. For more detailed hyperparameters and implementation details, see GitHub: https://github.com/sheng-n/DLST-MDA.

Evaluation strategies: In this study, the 5-fold cross-validation (5-cv) strategy is adopted to evaluate the performance of DLST-MDA and the baseline method on the benchmark dataset. Specifically, all known MDAs are regarded as positive samples, while all unknown MDAs are used as candidate negative samples set. DLST-MDA selected an equal number of negative samples from this candidate set to match the number of positive samples, ensuring a balanced dataset. The positive and selected negative samples are then randomly divided into 5 equal subsets. The validation process is repeated 5 times, with one subset reserved for testing and the remaining four used for training in each iteration.

Evaluation metrics: MDA prediction can be considered a classification task, with the primary goal of determining whether there will be interactions between miRNAs and drugs. To evaluate measure the prediction performance of the DLST-MDA and the comparison methods, several widely-used classification metrics are applied: Accuracy (Acc), Matthews correlation coefficient (Mcc), Sensitivity (Sen), specificity (Spe), the area under the receiver

operating characteristic curve (AUC), the area under the receiver operating characteristic curve (AUPR).

Performance comparison with other methods

To validate the performance of the DLST-MDA, we evaluated the method based on benchmark dataset and compared with five competitive methods, including DAESTB,[28] GCNNMMA[29], SubMDTA,[30] GraphDTA,[31] and ML-DTI.[32]

DAESTB integrates similarity and association matrices to construct small molecule-miRNA pair representation and extracted node pair features using an autoencoder. It then employs XGBoost to predict association scores between small molecules and miRNAs.

GCNNMMA applies CNNs and GNNs to learn miRNA sequence and drug structure feature, respectively, and predicts potential association scores using fully connected layer with an attention mechanism.

SubMDTA predicts drug-target affinity by integrating drug molecule graphs and target sequences. It extracts the molecule representation using GIN and adopts BiLSTM to obtain the protein sequence representation. Finally, the representations are concatenated and input into the fully connected layer to infer drug-target binding affinity. In our application, we input miRNA sequences and drug molecule graphs into the model to predict MDAs.

GraphDTA predicts drug-target affinity using a deep learning approach. It leverages graph neural networks for drug molecule feature extraction and CNNs for protein sequence embedding.

ML-DTI is a sequence-dependent drug-target interactions prediction method. Drug SMILES and protein sequences are encoded using 1D-CNN as encoder. A mutual learning layer bridges the two encoders, enabling the model to integrate the extracted features more effectively.

DLST-MDA is trained with other baseline methods at 5-cv strategy until convergence. Given that miRNA sequences are considerably shorter than protein sequences, we fine-tuned

Table 1: Performance comparison of DLST-MDA and comparison methods on benchmark dataset.

Methods	Acc	Mcc	Sen	Spe	AUC	AUPR
DAESTB	0.8447	0.6944	0.7954	**0.8939**	0.9279	0.9169
GCNNMMA	0.7615	0.6052	**0.9842**	0.6249	0.8630	0.7222
SubMDTA	0.8554	0.7109	0.8573	0.8536	0.9032	0.8659
GraphDTA	0.8478	0.7119	0.9537	0.7419	0.8692	0.8692
ML_DTI	0.6719	0.4284	0.7155	0.6802	0.7858	0.7058
DLST-MDA	**0.8736**	**0.7532**	0.9331	0.8130	**0.9411**	**0.9326**

the hyperparameters of the drug-target prediction models in the competing methods for the miRNA-drug prediction task. Table 1 and Figure 3 illustrates the experimental results of DLST-MDA as well as the baseline approach, from which we have the following observations: (1) DLST-MDA demonstrates superior performance on benchmark dataset, its AUC and AUPRC values are 0.9411 and 0.9326. Compared to the suboptimal models, DLST-MDA improves the AUC by 1.32% and the AUPR by 1.57%. (2) In contrast to DAESTM, a deep learning method that derives features from similarities, DLST-MDA directly extracts features from miRNA and drug sequences. This direct feature extraction proves more effective, likely due to its ability to capture intrinsic molecular characteristics that may be lost in similarity-based approaches. (3) DLST-MDA's performance highlights the importance of integrating both drug SMILES sequences and molecular graph information. This is evident when compared to GraphDTA and GCNNMMA, which utilizes only drug molecular graphs and miRNA sequences, and ML-DTI, which combines only miRNA and drug SMILES sequences. By leveraging both types of drug information, DLST-MDA achieves more comprehensive representation of drug properties, leading to improved prediction accuracy. (4) SubMDTA exhibits slightly inferior performances, possibly due to its reliance on LSTM for capturing long-distance information. While LSTM is typically effective for longer sequences like proteins, it may be counterproductive for the shorter miRNA sequences.

To summarize, we hypothesize that our model work well because the fusion of sequence and structural information, and the implementation of multi-scale CNN strategy also improves the results. Next, we will verify our conjecture through experiments.

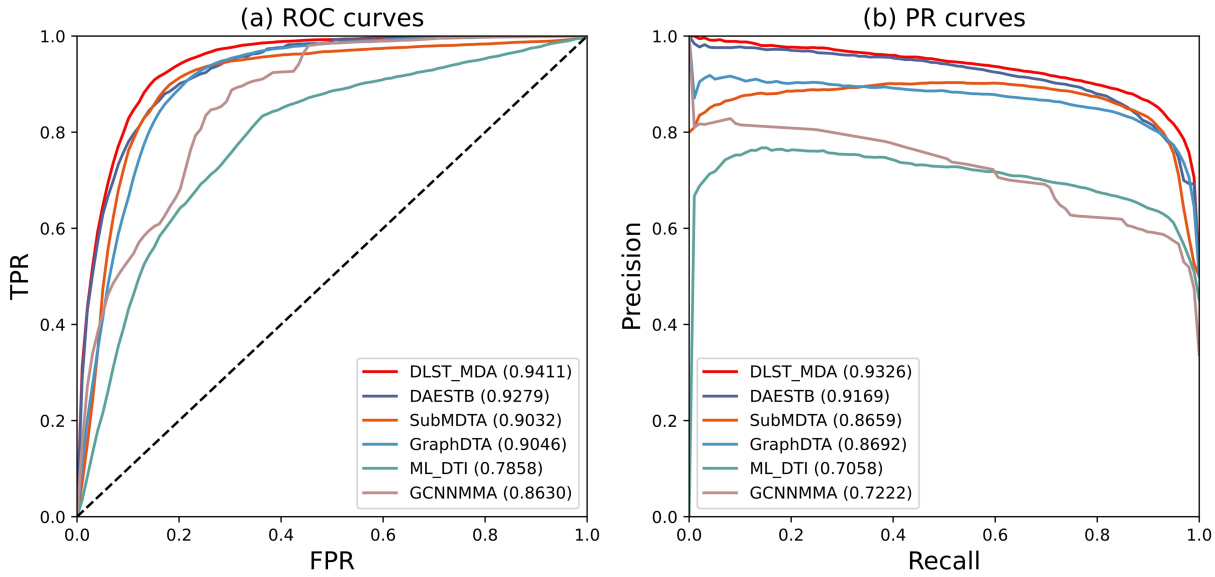

Figure 3: The ROC and PR curves of DLST-MDA as well as the baseline methods for MDA prediction.

Ablation experiment

In this section, to further investigate the importance of multi-scale CNN and the fusion of drug SMILES sequences and molecule graphs. We designed three variants of DLST-MDA: (1) DLST-MDA (w/o MC): without multi-scale CNN layer. (2) DLST-MDA (w/o DS): without drug SIMLES sequence. (3) DLST-MDA (w/o DG): without drug molecule graph. We performed ablation studies on the benchmark dataset, and the results are depicted in Figure 4.

Several key observations can be drawn from Figure 4, as follows: (1) The results of DLST-MDA consistently outperform three variants, demonstrating the validity and necessity of each component in the model. (2) The performance of DLST-MDA (w/o DS) and DLST-MDA (w/o DG) indicates that both drug SMILES sequence and molecular graph information contribute to performance. Especially the latter contain more drug features that are favorable for decision-making. (3) The inferior performance of DLST-MDA (w/o MC) confirms the value of multi-scale CNN, which can capture a wider range of node sequence features at various levels of granularity.

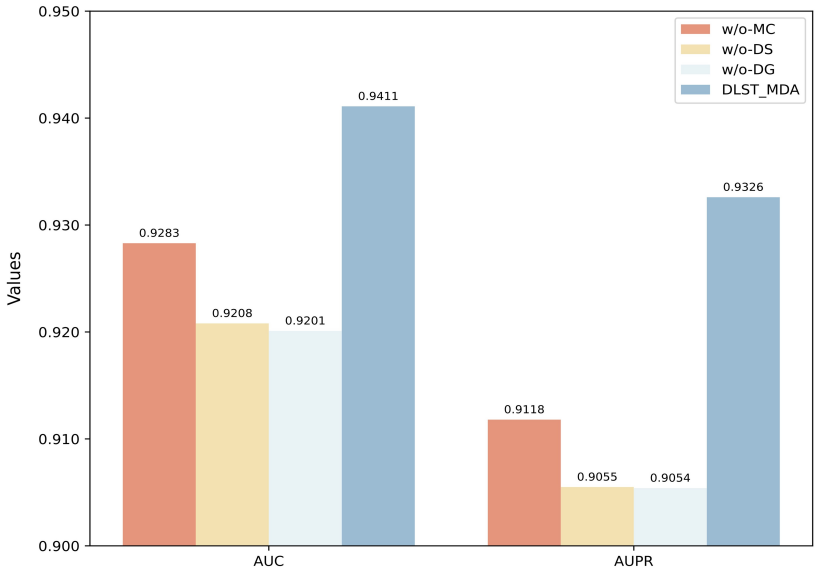

Figure 4: The comparison of DLST-MDA and its variants.

Analysis of hyperparameters

This section systematically evaluates the sensitivity of two main parameters in DLST-MDA: the embedding layer dimension $em(ed)$ of miRNAs and drugs and the multi-scale convolutional kernel size k. We conducted experiments using the benchmark dataset and reported the AUC and AUPR values, as shown in Figure 5.

Analysis of $em(ed)$: The initial embedding layer dimension $em(ed)$ is varied among of 32, 64, 128, 256, 512, and corresponding results are shown in Figure 5(a). As the increase of $em(ed)$, the performance goes up first and then declines. The optimal value is found to be 64. **Analysis of k:** The combination of multi-scale convolutional kernel sizes k determines the receptive field. Different values of k are tested and the corresponding results are presented in Figure 5(b). A notable trend emerges where model performance initially improves with larger convolution kernel sizes k, but eventually deteriorates. The best performance is achieved by DLST-MDA when the combination of kernel sizes 2, 3, and 4 is chosen. This phenomenon may be attributed to the relatively short of miRNA and drug sequences, which are not well-suited for feature extraction using larger convolution kernels. **Analysis of *epoch*:** The number of training epochs is varied from 10 to 50. The experimental results are presented

in Fig. 5(c). As the number of epochs increased, performance initially improved and then declined, with the optimal value determined to be 30. **Analysis of** lr: We tested the effect of learning rate lr, and vary it from 0.001 to 0.0001. The results shown in Fig. 5(d) demonstrate that optimal performance are achieved with the learning rate is 0.0005.

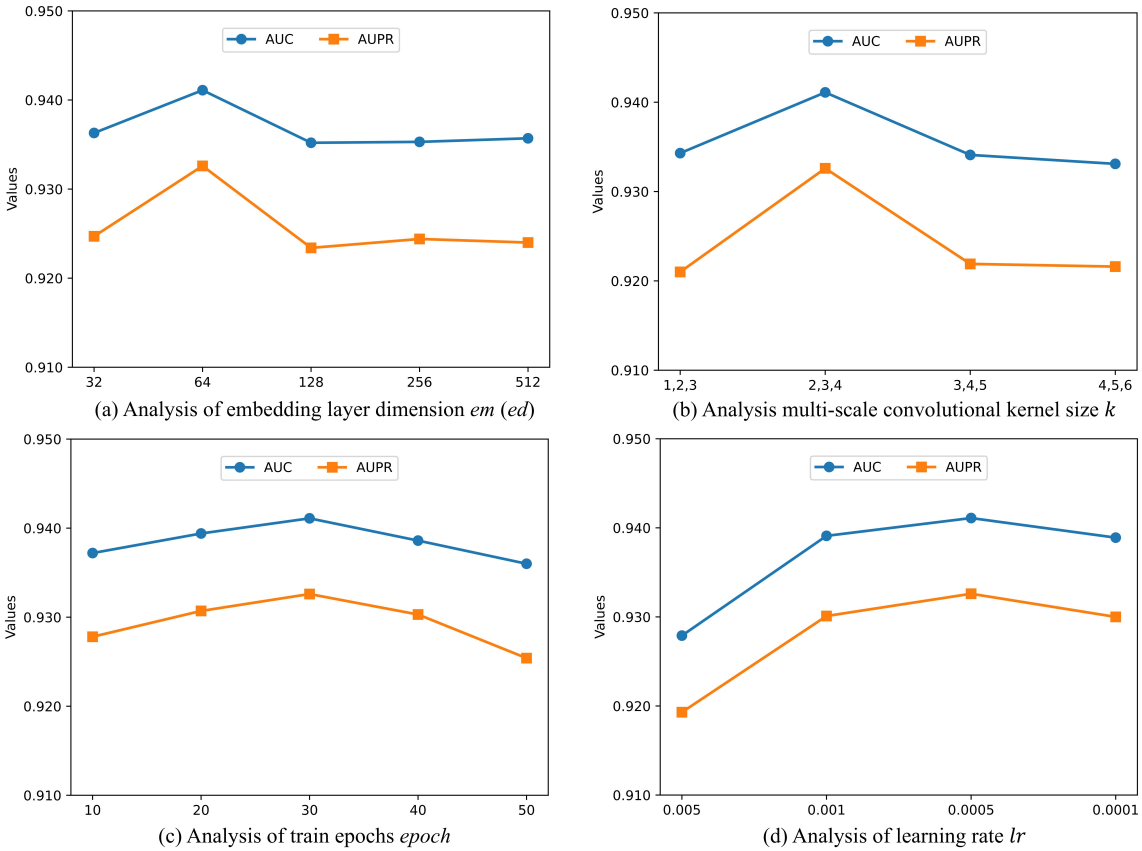

Figure 5: Analysis of (a) the embedding layer dimension $em(ed)$ and (b) the multi-scale convolutional kernel size.

Impact of negative samples

For the benchmark dataset, there are (1578×156)-8720=237448 negative examples. We evaluated DLST-MDA's prediction performance using different ratios of positive to negative samples. The results, shown in Table 2, indicate that as the number of negative samples increases, the model's accuracy/specificity improve, primarily because the model becomes more likely to predict negative classifications. Following previous studies,[20,33] we selected a

1:1 ratio for our experiments to maintain class balance.

Table 2: Performance evaluation of different positive vs negative sample ratios.

Ratio	Acc	Mcc	Sen	Spe	AUC	AUPR
1:1	0.8755	0.7545	0.9234	0.8268	0.9411	0.9326
1:5	0.9069	0.6794	0.7700	0.9344	0.9510	0.8026
1:10	0.9365	0.5891	0.5677	0.9734	0.9514	0.7049

Case studies: paclitaxel, oxaliplatin and doxorubicin

To verify the capability of DLST-MDA in discovering novel MDAs, we conduct case studies using three antitumor drugs: paclitaxel (DB01229), oxaliplatin (DB00526), and doxorubicin (DB00997). Our goal is to identify potential miRNAs that may influence drug resistance or sensitivity. Specifically, all known MDAs and unknown MDAs are used for training and testing, respectively. Candidate miRNAs are then ranked in descending order depending on DLST-MDA prediction scores. We selected the top 10 drug-related miRNAs for each drug and validated them against recent literature. Table 3 presents the results of these case studies.

Paclitaxel is a class of natural products that are widely utilized in the treatment of ovarian, breast and lung cancer. Recent studies have shown that miRNAs can exert both stimulatory and inhibitory effects on paclitaxel resistance by modulating the expression of genes such as YES1, SK2, MRP1, and STAT3.[34] Our analysis identified top 10 candidate miRNAs associated with paclitaxel, 5 of which are corroborated by existing literature (see Table 3). Importantly, 4 of the top 5 candidates have been supported by experimental verification. Notably, Yu et al. demonstrated that miR-520a-3p, our highest-ranked candidate, increased the sensitivity of NSCLC A549/TAX cells to paclitaxel by targeting FZD8, as verified through dual luciferase reporter gene assay.[35] Furthermore, in 2024 Vasconcelos et al. conducted a study analyzing blood samples from lung cancer patients before and after chemotherapy with a combination of carboplatin and paclitaxel. The results showed that miR-455-3p (third-ranked) was the most significant predictor of anemia in these patients.[36]

Table 3: The top 10 predicted paclitaxel, oxaliplatin, and doxorubicin-related miRNAs.

Drug names	Rank	miRNA names	Evidences
Paclitaxel	1	miR-520a-3p	DOI: 10.3872/j.issn.1007-385X.2019.10.009
	2	miR-184	Unconfirmed
	3	miR-455-5p	PMID: 38586206
	4	miR-124-3p	PMID: 31793989
	5	miR-153-3p	PMID: 37164696
	6	miR-454-3p	Unconfirmed
	7	miR-206	PMID: 29971911
	8	miR-1289	Unconfirmed
	9	miR-505-3p	Unconfirmed
	10	miR-323a-3p	Unconfirmed
Oxaliplatin	1	miR-210-3p	Unconfirmed
	2	miR-146a-5p	PMID: 26396533
	3	miR-193b-5p	Unconfirmed
	4	miR-146b-5p	PMID: 29888105
	5	miR-134-5p	PMID: 29041002
	6	miR-148a-3p	Unconfirmed
	7	miR-187-3p	PMID: 35954265
	8	miR-520a-3p	Unconfirmed
	9	miR-140-5p	PMID: 36324569
	10	miR-452-5p	PMID: 31810268
Doxorubicin	1	miR-24-3p	PMID: 27681638
	2	miR-1287-5p	Unconfirmed
	3	miR-663a	Unconfirmed
	4	miR-1289	Unconfirmed
	5	miR-24-2-5p	Unconfirmed
	6	miR-449a	PMID: 39174500
	7	miR-363-5p	PMID: 30037365
	8	miR-671-5p	PMID: 37939881
	9	miR-744-5p	Unconfirmed
	10	miR-3116	Unconfirmed

Oxaliplatin is a broadly used anticancer drug that typically employed in the treatment of colon, rectal, and stomach cancers. A case study of oxaliplatin is conducted performing DLST-MDA (see Table 3). The analysis revealed that 6 of the top 10 miRNA candidates can be validated through existing literature. In Chinese gastric cancer patients, Liao et al. demonstrated that miR-146a might correlate with lymph node metastasis and predict prognosis, who underwent surgical resection followed by treatment with oxaliplatin and fluoropyrimidines.[37] In addition, the doxorubicin is indicated for the treatment of various cancers, including breast, lung, and gastric cancers. Table 3 presents the top 10 predicted drug candidates for doxorubicin, of which 4 can be confirmed by previous publications. For example, Sun et al. revealed that miR-24 inhibitors were able to re-sensitize doxorubicin-resistant cells to doxorubicin.[38] The top three predicted miRNAs, miR-449a, miR-363-5p and miR-671-5p, have yet to be validated in the literature. Overall, the case studies of these three drugs further suggest that DLST-MDA has a good performance in identifying miRNA-mediated drugs.

Conclusion

In this paper, we present a deep learning method, DLST-MDA for identifying potential MDAs. Our approach fuses drug sequence and structural information, leveraging the intrinsic attributes of both miRNAs and drugs rather than relying on interaction graph. DLST-MDA performs multi-scale CNN to extract multi-granularity node embeddings from miRNAs and drug sequences. Additionally, it utilizes GCN to learn rich structural information from drug molecular graphs, capturing essential features that contribute to significantly improved prediction accuracy. Our experiments on curated benchmark datasets validate that DLST-MDA outperforms state-of-the-arts in MDAs prediction. Furthermore, the results of the case studies on antitumor drugs: paclitaxel, oxaliplatin, and doxorubicin are supported by the published literature, which underscoring the potential of the model in discovering novel

MDAs.

Despite its excellent performance, DLST-MDA has several limitations. (1) the current dataset contains relatively few known drugs, limiting the model's prediction performance for novel drugs. (2) efficiently integrating additional types of biological data to enhance the model's prediction capabilities remains a challenge for future work. In the future, we will further investigate the following two dimensions: (1) Extensibility studies: exploring the applicability of DLST-MDA to other types of non-coding RNA interactions, such as lncRNA-drug and circRNA-drug associations. (2) Interpretability enhancement: explaining why specific miRNAs are associated with drug resistance/sensitivity, thereby improving the model's interpretability and biological relevance.

ASSOCIATED CONTENT

Data and Software Availability

The data and source code are released at https://github.com/sheng-n/DLST-MDA.

Author Contributions

N.S. contributed to data curation, methodology, software development, and writing-original draft; Y.L. contributed to methodology and software development; L.G., L.W., and C.S. contributed to data curation and writing-review & editing; L.H. and Y.W. contributed to funding acquisition, supervision, writing - review & editing.

Conflicts of Interest

The authors declare no competing financial interest.

Acknowledgement

This work was supported by the National Natural Science Foundation of China (No.62072212, 62302218), the Jilin Provincial Scientific and Technological Development Program (No.20230201065GX, 20240101364JC) and the Jilin Provincial Key Laboratory of Big Data Intelligent Cognition (No.YDZJ202402075CXJD).

References

(1) F. Bray, M. Laversanne, E. Weiderpass, and I. Soerjomataram, "The ever-increasing importance of cancer as a leading cause of premature death worldwide," *Cancer*, vol. 127, no. 16, pp. 3029-3030, 2021.

(2) W. Si, J. Shen, H. Zheng, and W. Fan, "The role and mechanisms of action of microRNAs in cancer drug resistance," *Clin. Epigenetics*, vol. 11, no. 1, pp. 25, 2019.

(3) L. Wei, J. Sun, N. Zhang, Y. Zheng, X. Wang, L. Lv, J. Liu, Y. Xu, Y. Shen, and M. Yang, "Noncoding RNAs in gastric cancer: implications for drug resistance," *Mol. Cancer*, vol. 19, no. 1, pp. 62, 2020.

(4) M. Zhu, X. Zhou, Y. Du, Z. Huang, J. Zhu, J. Xu, G. Cheng, Y. Shu, P. Liu, W. Zhu, and T. Wang, "miR-20a induces cisplatin resistance of a human gastric cancer cell line via targeting CYLD," *Mol Med Rep*, vol. 14, no. 2, pp. 1742-1750, 2016.

(5) Y. Wu, W. Xu, Y. Yang, and Z. Zhang, "miRNA-93-5p promotes gemcitabine resistance in pancreatic cancer cells by targeting the PTEN-mediated PI3K/Akt signaling pathway," *Ann. Clin. Lab. Sci.*, vol. 51, no. 3, pp. 310-320, 2021.

(6) S. Safaei, M. Amini, S. Najjary, A. Mokhtarzadeh, N. Bolandi, H. Saeedi, N. Alizadeh, D. Javadrashid, and B. Baradaran, "miR-200c increases the sensitivity of breast cancer

cells to Doxorubicin through downregulating MDR1 gene," *Exp. Mol. Pathol.*, vol. 125, pp. 104753, 2022.

(7) L. Jiang, Y. Zhang, L. Guo, C. Liu, P. Wang, and W. Ren, "Exosomal microRNA-107 reverses chemotherapeutic drug resistance of gastric cancer cells through HMGA2/mTOR/P-gp pathway,"*BMC Cancer*, vol. 21, no. 1, pp. 1290, 2021.

(8) L. Li, P. Wu, Z. Wang, X. Meng, C. Zha, Z. Li, T. Qi, Y. Zhang, B. Han, S. Li, C. Jiang, Z. Zhao, and J. Cai, "NoncoRNA: a database of experimentally supported non-coding RNAs and drug targets in cancer," *J. Hematol. Oncol.*, vol. 13, no. 1, pp. 15, 2020.

(9) X. Cao, X. Zhou, F. Hou, Y.-e. Huang, M. Yuan, M. Long, S. Chen, W. Lei, J. Zhu, J. Chen, T. Zhang, A.-Y. Guo, and W. Jiang, "ncRNADrug: a database for validated and predicted ncRNAs associated with drug resistance and targeted by drugs," *Nucleic Acids Res.*, vol. 52, no. D1, pp. D1393-D1399, 2023.

(10) L. Huang, N. Sheng, L. Gao, L. Wang, W. Hou, J. Hong, and Y. Wang, "Self-Supervised Contrastive Learning on Attribute and Topology Graphs for Predicting Relationships Among lncRNAs, miRNAs and Diseases," *IEEE Journal of Biomedical and Health Informatics*, vol. 29, no. 1, pp. 657-668, 2025.

(11) X. Liang, M. Guo, L. Jiang, Y. Fu, P. Zhang, and Y. Chen, "Predicting miRNA–Disease Associations by Combining Graph and Hypergraph Convolutional Network," *Interdisciplinary Sciences: Computational Life Sciences*, vol. 16, no. 2, pp. 289-303, 2024.

(12) W. Yin, S. Wang, S. Qiao, Y. Zhao, W. Wu, S. Pang, and Z. Lv, "DETHACDA: A Dual-View Edge and Topology Hybrid Attention Model for CircRNA-Disease Associations Prediction," *IEEE Journal of Biomedical and Health Informatics*, vol. 28, no. 8, pp. 4421-4431, 2024.

(13) S. Lei, X. Lei, M. Chen, and Y. Pan, "Drug Repositioning Based on Deep Sparse

Autoencoder and Drug–Disease Similarity," *Interdisciplinary Sciences: Computational Life Sciences*, vol. 16, no. 1, pp. 160-175, 2024.

(14) Y. Wang, J. Song, M. Wei, and X. Duan, "Predicting Potential Drug–Disease Associations Based on Hypergraph Learning with Subgraph Matching," *Interdisciplinary Sciences: Computational Life Sciences*, vol. 15, no. 2, pp. 249-261, 2023.

(15) Y.-a. Huang, P. Hu, K. C. C. Chan, and Z.-H. You, "Graph convolution for predicting associations between miRNA and drug resistance," *Bioinformatics*, vol. 36, no. 3, pp. 851-858, 2019.

(16) Y. Li, R. Wang, S. Zhang, H. Xu, and L. Deng, "LRGCPND: Predicting Associations between ncRNA and Drug Resistance via Linear Residual Graph Convolution," *Int. J. Mol. Sci.*, 22, 2021.

(17) Y. Niu, C. Song, Y. Gong, and W. Zhang, "MiRNA-Drug Resistance Association Prediction Through the Attentive Multimodal Graph Convolutional Network," *Front. Pharmacol.*, vol. 12, 2022.

(18) S.-H. Wang, C.-C. Wang, L. Huang, L.-Y. Miao, and X. Chen, "Dual-Network Collaborative Matrix Factorization for predicting small molecule-miRNA associations," *Brief. Bioinform.*, vol. 23, no. 1, 2021.

(19) L. Deng, Z. Fan, X. Xiao, H. Liu, and J. Zhang, "Dual-Channel Heterogeneous Graph Neural Network for Predicting microRNA-Mediated Drug Sensitivity," *J. Chem Inf. Model.*, vol. 62, no. 23, pp. 5929-5937, 2022.

(20) J. Wei, L. Zhuo, Z. Zhou, X. Lian, X. Fu, and X. Yao, "GCFMCL: predicting miRNA-drug sensitivity using graph collaborative filtering and multi-view contrastive learning," *Brief. Bioinform.*, vol. 24, no. 4, 2023.

(21) Z. Zhou, Z. Du, X. Jiang, L. Zhuo, Y. Xu, X. Fu, M. Liu, and Q. Zou, "GAM-MDR: probing miRNA–drug resistance using a graph autoencoder based on random path masking," *Brief. Funct. Genomics*, vol. 23, no. 4, pp. 475-483, 2024.

(22) D. Ouyang, B. Jin, J. Tian, P. Duan, L. Lin, X. Zhu, S. Fan, R. Miao, and N. Ai, "MGHSTCKW: Predicting miRNA–drug sensitivity association using hypergraph sparse transformer and hypergraph-induced contrastive learning based on meta-path," *Expert Systems with Applications*, vol. 274, pp. 126879, 2025.

(23) Y. Fan, C. Zhang, X. Hu, Z. Huang, and L. Deng, "AGCLNDA: Enhancing the Prediction of ncRNA-Drug Resistance Association Using Adaptive Graph Contrastive Learning," *IEEE Journal of Biomedical and Health Informatics*, pp. 1-10, 2025.

(24) Y. Li, S. Wang, Y. Zhang, C. Ren, T. Liu, Y. Liu, and S. Pang, "IRPCA: An Interpretable Robust Principal Component Analysis Framework for Inferring miRNA–Drug Associations," *Journal of Chemical Information and Modeling*, vol. 65, no. 5, pp. 2432-2442, 2025.

(25) A. Kozomara, M. Birgaoanu, and S. Griffiths-Jones, "miRBase: from microRNA sequences to function," *Nucleic Acids Res.*, vol. 47, no. D1, pp. D155-D162, 2018.

(26) C. Knox, M. Wilson, Christen M. Klinger, M. Franklin, E. Oler, A. Wilson, A. Pon, J. Cox, N. E. Chin, Seth A. Strawbridge, M. Garcia-Patino, R. Kruger, A. Sivakumaran, S. Sanford, R. Doshi, N. Khetarpal, O. Fatokun, D. Doucet, A. Zubkowski, Dorsa Y. Rayat, H. Jackson, K. Harford, A. Anjum, M. Zakir, F. Wang, S. Tian, B. Lee, J. Liigand, H. Peters, R. Q. Wang, T. Nguyen, D. So, M. Sharp, R. da Silva, C. Gabriel, J. Scantlebury, M. Jasinski, D. Ackerman, T. Jewison, T. Sajed, V. Gautam, and David S. Wishart, "DrugBank 6.0: the DrugBank Knowledgebase for 2024," *Nucleic Acids Res.*, vol. 52, no. D1, pp. D1265-D1275, 2023.

(27) T. N. Kipf, and M. Welling, "Semi-Supervised Classification with Graph Convolutional Networks," *in International Conference on Learning Representations*, 2017.

(28) L. Peng, Y. Tu, L. Huang, Y. Li, X. Fu, and X. Chen, "DAESTB: inferring associations of small molecule–miRNA via a scalable tree boosting model based on deep autoencoder," *Brief. Bioinform.*, vol. 23, no. 6, 2022.

(29) Z. Niu, X. Gao, Z. Xia, S. Zhao, H. Sun, H. Wang, M. Liu, X. Kong, C. Ma, H. Zhu, H. Gao, Q. Liu, F. Yang, X. Song, J. Lu, and X. Zhou, "Prediction of small molecule drug-miRNA associations based on GNNs and CNNs," *Frontiers in Genetics*, vol. 14, 2023.

(30) S. Pan, L. Xia, L. Xu, and Z. Li, "SubMDTA: drug target affinity prediction based on substructure extraction and multi-scale features," *BMC Bioinformatics*, vol. 24, no. 1, pp. 334, 2023.

(31) T. Nguyen, H. Le, T. P. Quinn, T. Nguyen, T. D. Le, and S. Venkatesh, "GraphDTA: predicting drug–target binding affinity with graph neural networks," *Bioinformatics*, vol. 37, no. 8, pp. 1140-1147, 2020.

(32) Z. Yang, W. Zhong, L. Zhao, and C. Y.-C. Chen, "ML-DTI: Mutual Learning Mechanism for Interpretable Drug–Target Interaction Prediction," *The Journal of Physical Chemistry Letters*, vol. 12, no. 17, pp. 4247-4261, 2021.

(33) J. Zheng, Y. Qian, J. He, Z. Kang, and L. Deng, "Graph Neural Network with Self-Supervised Learning for Noncoding RNA–Drug Resistance Association Prediction," *Journal of Chemical Information and Modeling*, vol. 62, no. 15, pp. 3676-3684, 2022.

(34) M. K. Mahabady, S. Mirzaei, H. Saebfar, M. H. Gholami, A. Zabolian, K. Hushmandi, F. Hashemi, F. Tajik, M. Hashemi, A. P. Kumar, A. R. Aref, A. Zarrabi, H. Khan, M. R. Hamblin, Y. Nuri Ertas, and S. Samarghandian, "Noncoding RNAs and their

therapeutics in paclitaxel chemotherapy: Mechanisms of initiation, progression, and drug sensitivity," *J. Cell. Physiol.*, vol. 237, no. 5, pp. 2309-2344, 2022.

(35) X. YU, X. LI, X. QIAN, J. LIU, and H. ZHENG, "miR-520a-3p enhances the paclitaxel sensitivity of non-small cell lung cancer A549/TAX cells by targeting FZD8," *Chinese Journal of Cancer Biotherapy*, vol. 6, pp. 1107-1112, 2019.

(36) P. E. N. S. Vasconcelos, C. S. Seguin, A. D. S. Barbeiro, L. Zambon, H. N. Honma, A. W. Perroud Jr, M. V. Geraldo, E. D. C. Pincinato, and P. Moriel, "hsa-miR-455-3P as a predictive biomarker of anemia in patients with non-small cell lung cancer treated with carboplatin plus paclitaxel," *Oncol. Lett.*, vol. 27, no. 5, pp. 219, 2024.

(37) Y.-Q. Liao, Y.-L. Liao, J. Li, L.-X. Peng, Y.-Y. Wan, and R. Zhong, "Polymorphism in miR-146a associated with clinical characteristics and outcomes in gastric cancer patients treated with adjuvant oxaliplatin and fluoropyrimidines," *OncoTargets Ther.*, vol. 8, no. null, pp. 2627-2633, 2015.

(38) Y. Sun, N. He, Y. Dong, and C. Jiang, "MiR-24-BIM-Smac/DIABLO axis controls the sensitivity to doxorubicin treatment in osteosarcoma," *Scientific Reports*, vol. 6, no. 1, pp. 34238, 2016.

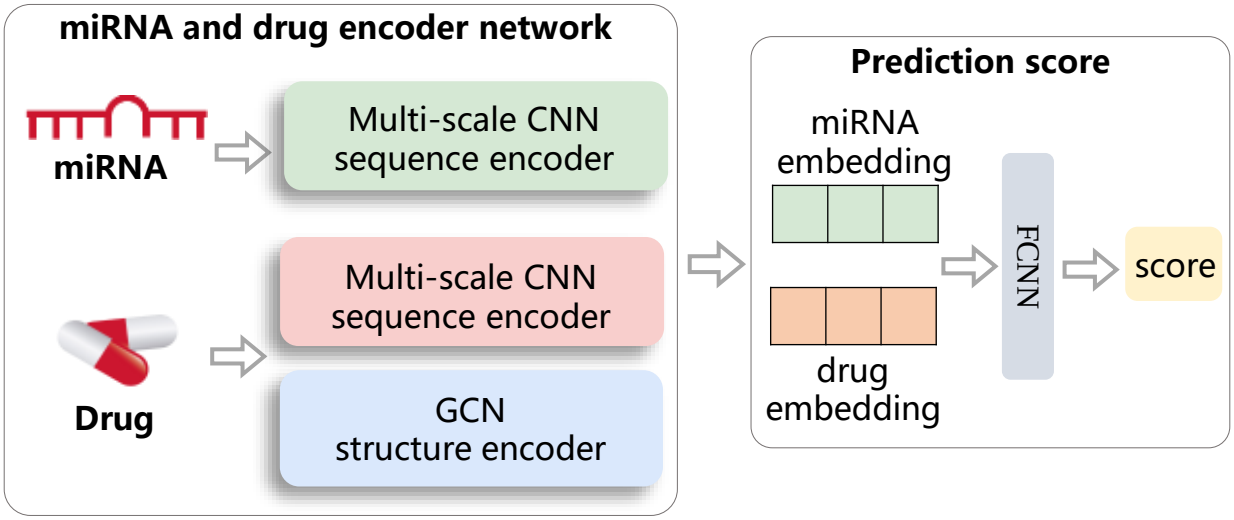

Figure 6: Table of Contents (TOC) Graphic for DLST-MDA